EVALUATION OF DISCHARGE HYDROGRAPHS AND FLOOD STORAGE IN THE MAIN RIVER AND TRIBUTARY CONFLUENCE

Shoji Fukuoka[1] and Hiroaki Sato[2]

ABSTRACT

Rivers possesses the function of storage and peak discharge attenuation of flood water. Author's recent studies have deepened basic understanding of these important characteristics of the flood flow. At the river confluence, downstream boundary conditions of a tributary change with temporary change in water level of the main river. Waters flowing down the tributary and transmitted back into the tributary from the main river are stored in the tributary section.

Furthermore, at the river confluence, a water level changes with time and adverse water surface slope occurs under the temporal change in the downstream boundary conditions. To estimate accurate discharge hydrographs under such complicated hydraulic conditions is important for the river planning of the main river and tributary. The authors, focusing on the confluence between the Tone and Watarase Rivers—for which temporally detailed flood level hydrographs were available—decided to use two-dimensional unsteady-flow analysis to re-create the temporal changes in water surface profile with the goal of creating highly precise estimated discharge hydrographs and storage rate for the main river–tributary confluence.

Key Words : *water surface profile, flood discharge hydrograph, flood storage volume*

1. INTRODUCTION

It has long been known that as a flood flow having a temporally variable discharge travels downstream, storage of the floodwaters occurs according to the planform and cross-sectional form of the channel, resulting in the attenuation of peak discharge and hydrograph transformation (Nomitsu 1964, Fukuoka 2005). Fukuoka and Watanabe (2003) arrived at a fundamental understanding of this storage phenomenon by conducting a series of experimental investigations from the viewpoint that estimating both the transformation of flood discharge hydrographs and the attenuation of peak discharge is of great significance, and that storage volume should be quantitatively assessed and incorporated into river planning. In addition, Fukuoka and Watanabe (2004a) using the two-dimensional unsteady-flow analysis that emphasizes temporal change in water surface profile, have made highly precise estimates of discharge hydrographs and channel storage in the Edo and Maruyama Rivers on the basis of longitudinally detailed observed water-level hydrograph data. Fukuoka and Watanabe (2004b) have also investigated the issue of

[1] Professor, Research and Development Initiative, Chuo University, 1-13-27 Kasuga Bunkyo-ku Japan (sfuku@tamacc.chuo-u.ac.jp)
[2] Director, Foundation of River Basin Integrated Communications, Japan, 1-3 Koujimachi Chiyoda-ku Japan (hi-sato @ river.or.jp)

measuring water level at practical longitudinal intervals, and have found that an interval of 3 to 4 km would yield a discharge hydrograph of sufficient precision.

One-dimensional unsteady-flow analysis, which is widely used in such cases, is capable of incorporating the effects of storage arising from the unsteadiness of flood flows but cannot adequately account for two-dimensional behavior of flood. For instance, it is difficult for the technique to assess, with a high degree of precision, flood discharge hydrographs and storage volume arising from irregularity in a channel's profile and cross-section. Consequently, at the very least, two-dimensional unsteady-flow analysis is needed to describe vividly changes in flood discharge hydrograph and storage in a watercourse with a complex planform. (Fukuoka 2005)

At the confluence of a main river and tributary whose downstream-end boundary conditions change temporally, flow retention occurs in the section of the tributary affected by confluence water level, resulting in overlapping of the flow from the tributary's upstream reaches and the flow transmitted back into the tributary from the main river. Because tributary water level at such a confluence changes temporally (including taking on a negative water surface slope) due to the downstream-end boundary conditions, high-precision estimated discharge hydrographs for such tributaries were considered difficult to generate. Therefore, The authors, focusing on the confluence between the Tone and Watarase Rivers—for which temporally detailed flood level hydrographs were available—decided to use two-dimensional unsteady-flow analysis to re-create the temporal changes in water surface profile with the goal of creating highly precise estimated discharge hydrographs and storage rate for the main river–tributary confluence.

2. METHOD OF ANALYSIS

Velocity, water level, and other quantities used in the analysis were determined using equations of motion (1) and (2) and continuity equation (3) below in a physical component representation form based on a general coordinate system. The method of calculation is the same as that used by Fukuoka and Watanabe (2004a).

$$\frac{\partial \tilde{U}}{\partial t}h+\tilde{U}h\{\frac{\partial \tilde{U}}{\partial \tilde{\xi}}-\tilde{J}(\tilde{V}-\tilde{U}\cos\theta^{\eta\xi})\frac{\partial \theta^{\xi}}{\partial \tilde{\xi}}\}+\tilde{V}h\{\frac{\partial \tilde{U}}{\partial \tilde{\eta}}-\tilde{J}(\tilde{V}-\tilde{U}\cos\theta^{\eta\xi})\frac{\partial \theta^{\xi}}{\partial \tilde{\eta}}\}=-gh\{\frac{\partial \zeta}{\partial \tilde{\xi}}+\cos\theta^{\eta\xi}\frac{\partial \zeta}{\partial \tilde{\eta}}\}-\tau_{z\xi}$$
$$+\frac{1}{J}[\frac{\partial}{\partial \xi}(\frac{Jh}{d\xi}\tilde{\tau}_{\xi\xi})+\frac{\partial}{\partial \eta}(\frac{Jh}{d\eta}\tilde{\tau}_{\xi\eta})]-\tilde{J}h(-\tilde{\tau}_{\xi\xi}\cos\theta^{\eta\xi}+\tilde{\tau}_{\xi\eta})\frac{\partial \theta^{\xi}}{\partial \tilde{\xi}}-\tilde{J}h(-\tilde{\tau}_{\xi\eta}\cos\theta^{\eta\xi}+\tilde{\tau}_{\eta\eta})\frac{\partial \theta^{\xi}}{\partial \tilde{\eta}} \tag{1}$$

$$\frac{\partial \tilde{V}}{\partial t}h+\tilde{U}h\{\frac{\partial \tilde{V}}{\partial \tilde{\xi}}+\tilde{J}(\tilde{U}-\tilde{V}\cos\theta^{\eta\xi})\frac{\partial \theta^{\eta}}{\partial \tilde{\xi}}\}+\tilde{V}h\{\frac{\partial \tilde{V}}{\partial \tilde{\eta}}+\tilde{J}(\tilde{U}-\tilde{V}\cos\theta^{\eta\xi})\frac{\partial \theta^{\eta}}{\partial \tilde{\eta}}\}=-gh\{\cos\theta^{\eta\xi}\frac{\partial \zeta}{\partial \tilde{\xi}}+\frac{\partial \zeta}{\partial \tilde{\eta}}\}-\tau_{z\eta}$$
$$+\frac{1}{J}[\frac{\partial}{\partial \xi}(\frac{Jh}{d\xi}\tilde{\tau}_{\eta\xi})+\frac{\partial}{\partial \eta}(\frac{Jh}{d\eta}\tilde{\tau}_{\eta\eta})]-\tilde{J}h(-\tilde{\tau}_{\xi\xi}+\tilde{\tau}_{\xi\eta}\cos\theta^{\eta\xi})\frac{\partial \theta^{\eta}}{\partial \tilde{\xi}}-\tilde{J}h(-\tilde{\tau}_{\xi\eta}+\tilde{\tau}_{\eta\eta}\cos\theta^{\eta\xi})\frac{\partial \theta^{\eta}}{\partial \tilde{\eta}} \tag{2}$$

$$J\frac{\partial h}{\partial t}+\frac{\partial}{\partial \xi}(\frac{J\tilde{U}h}{d\xi})+\frac{\partial}{\partial \eta}(\frac{J\tilde{V}h}{d\eta})=0 \tag{3}$$

$$\frac{\partial}{\partial \tilde{\xi}}=\frac{\partial}{d\xi\partial\xi}\qquad\frac{\partial}{\partial \tilde{\eta}}=\frac{\partial}{d\eta\partial\eta}$$

$$(\tau_{z\eta},\tau_{z\eta})=\left(\frac{gn^2}{h^{1/3}}+\frac{gh_a}{K^2}\right)\sqrt{u^2+v^2}\,(\tilde{U},\tilde{V}) \tag{4}$$
$$h_a=\min(h,h_{tree})\qquad u^2+v^2=\tilde{J}^2(\tilde{U}^2-2\tilde{U}\tilde{V}\cos\theta^{\eta\xi}+\tilde{V}^2)$$

where (ξ,η) is the general curvilinear coordinate system, $(d\xi,d\eta)$ is the contravariant distance, ~ is a physical component, $(\tilde{U},\tilde{V})$ is contravariant velocity, h is depth, $J = [x_\xi y_\eta - x_\eta y_\xi = 1/(\xi_x\eta_y - \xi_y\eta_x)]$ is the Jacobian, (θ^ξ,θ^η) is the angle of the x-axis in the contravariant coordinate system, $\theta^{\eta\xi}$ is the angle of intersection in the contravariant coordinate system, and $[\sqrt{u^2+v^2}]$ is absolute velocity. The shear stress terms $[\tau_{z\xi},\tau_{z\eta}]$ indicate bottom shear stress and fluid resistance of vegetation and are determined with equation (4) using Manning's roughness coefficient *n*, vegetation permeability coefficient *K*, and vegetation height h_{tree}. Convection terms are discretized as an upwind differential and indicated with first-order accuracy, as it includes the flood front inundating over the flood channel. The overall procedure of analysis is shown in the flowchart in Figure 1. Conventional unsteady-flow analysis is used to calculate temporal changes in water level and discharge from observed discharge and water level for the upstream and downstream ends, respectively, under the assumption that observed discharge is accurate. However, observed flood discharge is thought to contain more error than water surface profile determined from water level data simultaneously obtained at multiple locations. Consequently, in this analysis, the authors, assuming water profile to be more accurate than observed discharge, and using the same methodology employed previously by Fukuoka and Watanabe (2004a), back-calculated resistance coefficient distribution so that temporal changes in calculated discharge and water surface profile generally agree with the observed data, then used this estimated resistance coefficient distribution to determine the discharge hydrograph.

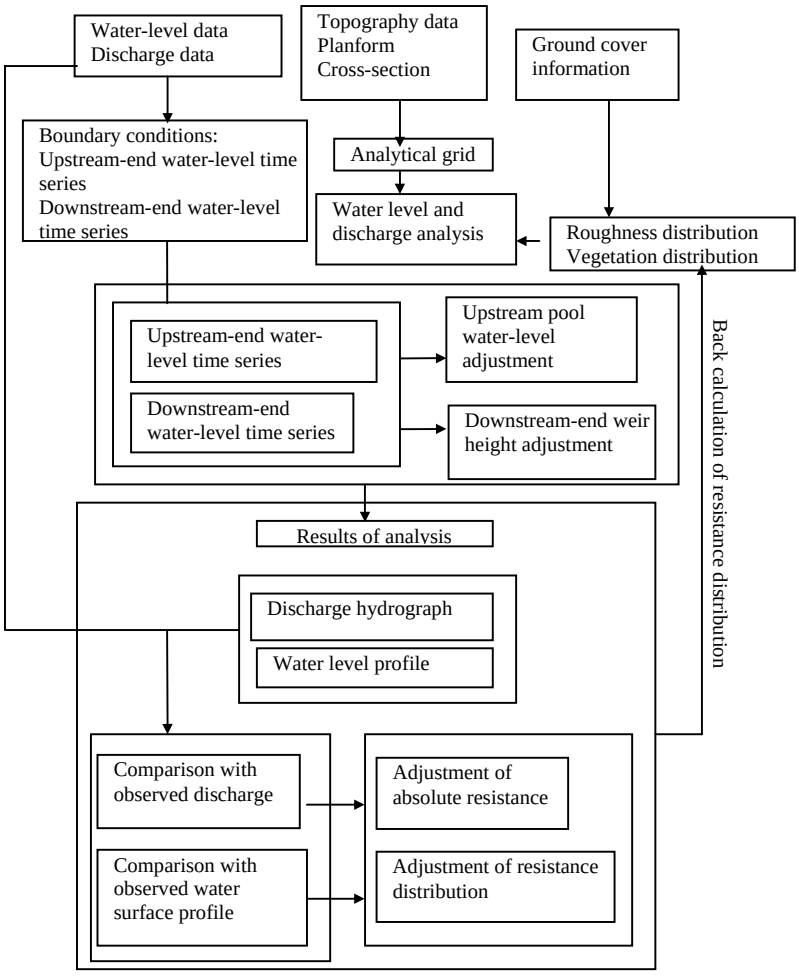

Figure 1. Flowchart of analysis.

3. ANALYSIS CONDITIONS FOR THE TONE AND WATARASE RIVERS

Figure 2 shows the planform and ground cover of the analyzed sections of the Tone and Watarase Rivers. The flood in these sections are primarily grassland, with generally sparse growth of taller vegetation, although the flood plain of the 128.0–129.5 km section of the Tone River contains dense vegetation. In addition, public-use areas have been established in the flood plain of both rivers, including downstream from the 130.0 km point of the Tone River, on the left bank. There is also a golf course on the left bank of the Watarase River, between the 3.5 and 5.0 km points.

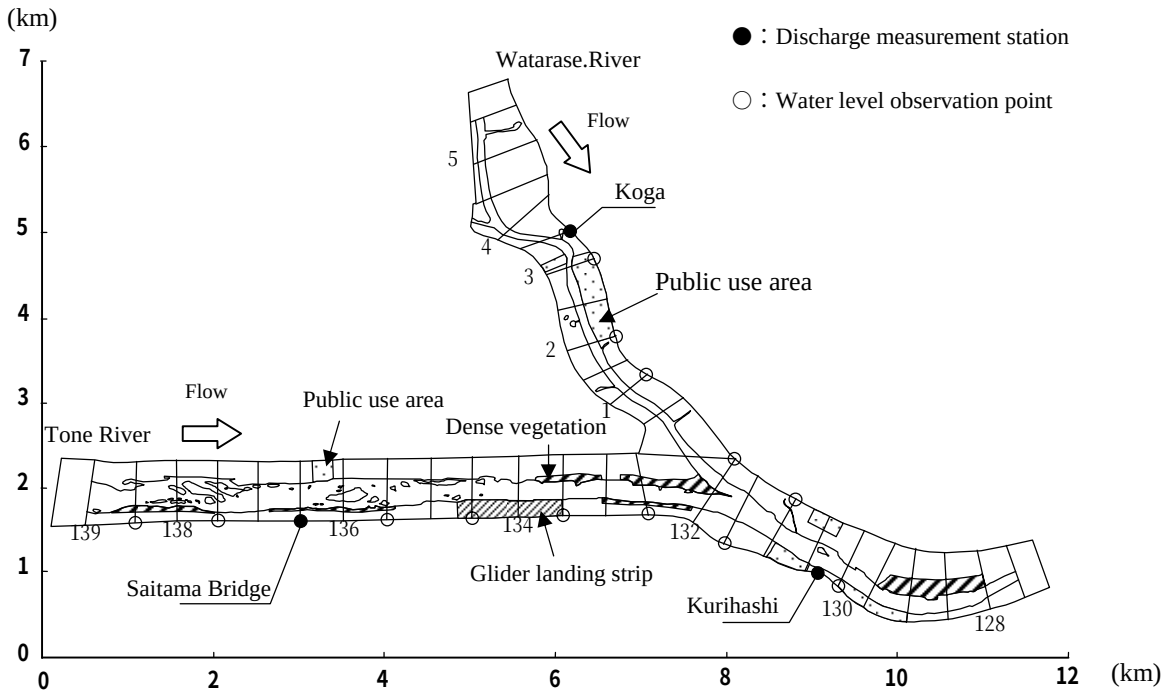

Figure 2 Planform and channel conditions of the studied sections.

Table-1 Roughness coefficient and vegetation permeability coefficient of the Tone River

Location		Roughness Coefficient
Main-channel		0.029
Flood-plain public use area		0.034
128.0-129.0	Right	0.039
	Left	0.048
129.0-130.0	Right	0.042
	Left	0.052
130.0-131.0	Right	0.042
	Left	0.045
131.0-132.0	Right	0.048
	Left	0.046
132.0-133.5	Right	0.048
	Left	0.048
133.5-135.5	Right	0.038
	Left	0.040
135.5-136.5	Right	0.040
	Left	0.036
136.5-139.0	Right	0.040
	Left	0.038

Location	Vegetation permeability coefficient (m/s)
128.0〜129.0 Right bank	42.0
129.0〜131.5 Right bank	48.0
131.5〜133.5 Right bank	52.0
133.5〜135.0 Right bank	50.0
135.0〜139.0 Right bank	52.0
128.0〜129.5 Left bank	33.5
129.5〜130.5 Left bank	42.0
130.5〜132.0 Left bank	38.0
132.0〜134.0 Left bank	48.0
134.0〜136.0 Left bank	46.0
136.0〜137.0 Left bank	48.0
137.0〜139.0 Left bank	44.0

Table-2 Roughness coefficient and vegetation permeability coefficient of the Watarase River

Location		Roughness Coefficient
Main-channel		0.029
Flood-plain public use area		0.034
0.0-2.0	Right	0.042
	Left	0.040
2.0-3.0	Right	0.038
	Left	0.036
3.0-4.0	Right	0.039
	Left	0.038
4.0-5.0	Right	0.038
	Left	0.036

Location	Vegetation permeability coefficient (m/s)
0.0〜2.0 Right bank	48.0
2.0〜3.0 Right bank	52.0
3.0〜4.0 Right bank	49.5
4.0〜5.0 Right bank	53.0
0.0〜2.0 Left bank	46.0
2.0〜3.0 Left bank	54.0
3.0〜5.0 Left bank	44.0
0.0〜2.0 Right bank	48.0
2.0〜3.0 Right bank	52.0
3.0〜4.0 Right bank	49.5
4.0〜5.0 Right bank	53.0
0.0〜2.0 Left bank	46.0

Water-level measuring points are indicated in the figure with hollow circles. Discharge is measured at three cross-sections: Saitama Bridge, Kurihashi, and Koga.

A trial-and-error approach was employed to determine the roughness coefficients and vegetation permeability coefficients used for the main channel and flood plain in the analysis. The values are listed in Table 1. The analytical grid is divided longitudinally into 372 cells for the Tone River and 180 cells for the Watarase River, and divided laterally into 20 cells for both rivers.

The flood studied was one that lasted for several days beginning on September 10, 2001 (see Figure 3). Discharge was measured at three locations—Koga and Saitama Bridge at the upstreamend and Kurihashi at the downstream end—approximately every 2 hour over a 48-hour period, from 8:00 p.m. September 10 to 8:00 p.m. September 12. Water level was measured approximately every hour at 1-km intervals in both rivers: on the right bank of the 130.0–138.5 km section of the Tone River and on the left bank of the 0–3.5 km section of the Watarase River. To improve the accuracy of calculations, the authors extended the target river section beyond the locations of the upstream (Watarase River) and downstream (Tone River) discharge measurement stations.

Analysis focused on the 48-hour period from 8:00 p.m. September 10 to

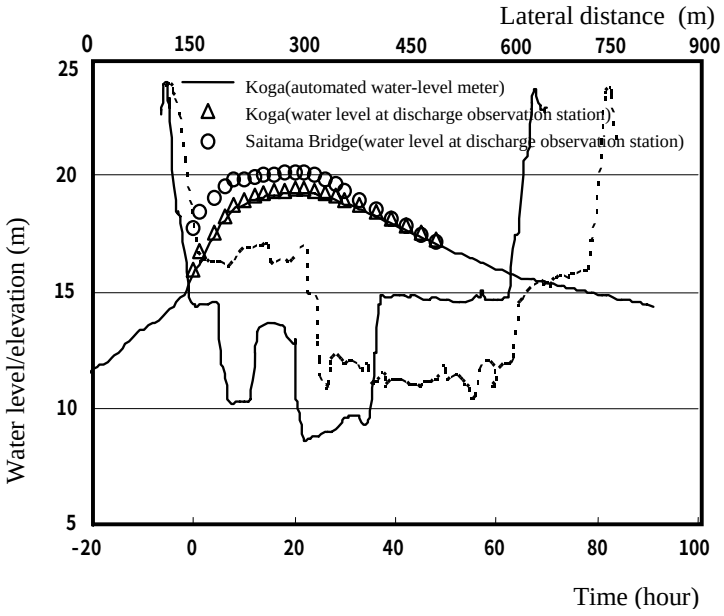

Figure 3(a). Observed water levels and cross-sections at discharge observation stations.

8:00 p.m. September 12. The former time, which marked the start of observations, was defined as the reference time.

Figure 3(a) and 3(b) show water level recorded by automated water-level meters, water level at discharge observation stations, and river cross-sections at the upstream end (Saitama Bridge and Koga) and the downstream end (Kurihashi).

The automated water-level meter data showed good agreement with the discharge observation station data at Koga and Kurihashi and were therefore used as the upstream and downstream end boundary conditions. Although no automated water-level meter was in place at Saitama Bridge, because of the agreement between the aforementioned data, we judged observation error to be slight and therefore used the Saitama Bridge discharge observation station data as the Tone River upstream end boundary condition(water level). When intensive observation began at 8:00 p.m. on the 10th, water level at Kurihashi was 15.5 m, already inundating the flood plain to a depth of roughly 1.0m. The flood plains throughout the observation section were similarly inundated.

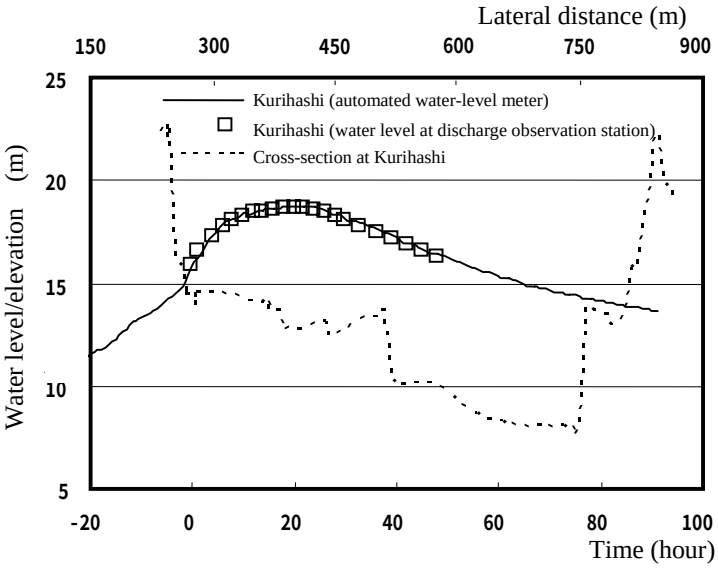

Figure 3(b). Observed water levels and cross-sections at discharge observation stations

4. ANALYSIS RESULTS AND CONSIDERATIONS

4.1 Water Level Profile

Figures 4(a) and 4(b) and Figures 5(a) and 5(b) show the temporal change in observed and calculated water level profile in the Tone and Watarase Rivers, respectively. Figures 4(a) and 5(a) show the rising-water period, Figures 4(b) and 5(b) the receding-water period. The calculated results for the studied section of the Tone River show good agreement with the observed results. Early in the rising-water period, as seen in Figure 4(a), water level remains essentially uniform near the 132.0 km point. This is believed to be due to the effect of outflow from the Watarase River, as the point in question is the confluence with the Watarase River. For the Watarase River section, too, the calculated results show good agreement with the observed data. The Watarase water surface profile changes due to the effect of the Tone River's water level. As Figure 5(a) shows, the calculations re-create the change from a negative water surface slope in the rising-water period to a gentle positive slope. Agreement is also good between water levels at the confluence—Tone River point 132.0 km and Watarase River point 0.0 km—indicating good connectivity at the confluence.

4.2 Comparison of Discharge Hydrographs

Figure 6 compares observed and calculated discharge at the Tone River's upstream- and downstream-end discharge observation points (Saitama Bridge and Kurihashi, respectively). Other than during the rising-water period, the discharge hydrographs exhibit good agreement.

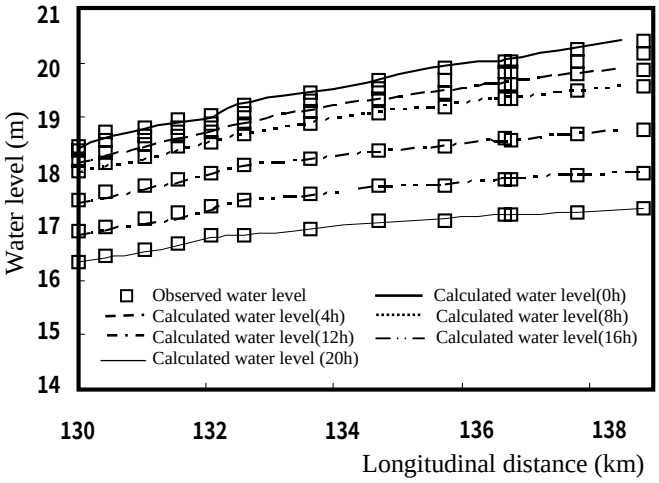

Figure4(a) Observed and calculated water levels

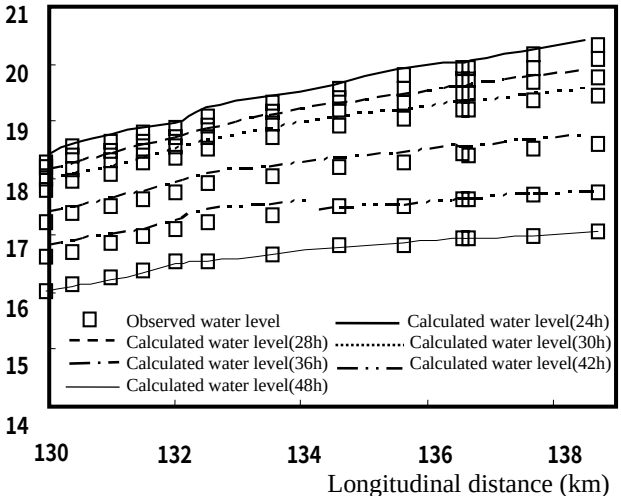

Figure4(b) Observed and calculated water levels (receding-water period; Tone River)

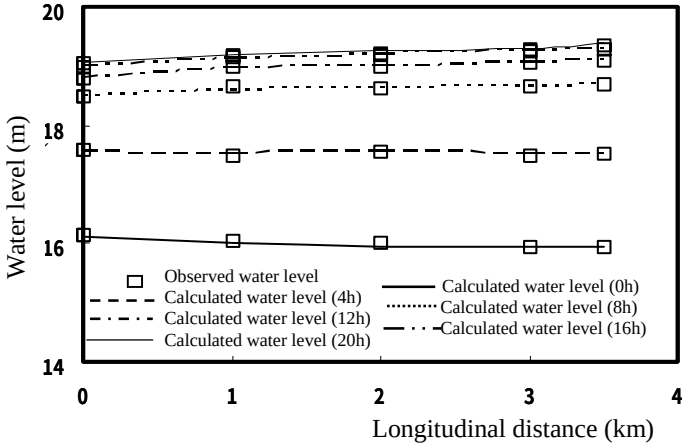

Figure5(a) Observed and calculated water levels (rising-water period; Watarase River)

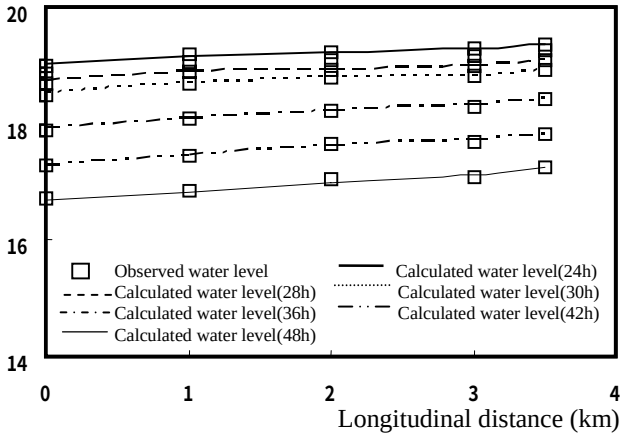

Figure5(b) Observed and calculated water levels (receding-water period; Watarase River)

Observed discharge in the rising-water period was measured using floats—a technique whose poor accuracy compared to results produced in receding-water periods has been seen in research on the Edo and Maruyama Rivers by Fukuoka and Watanabe (2004), suggesting that the same phenomenon is reflected in the authors' Tone River data. The poor accuracy in the rising-water period of a flood is because vegetation in the flood plain impedes the floats' flow, resulting in poor discharge accuracy. Starting around peak discharge, however, when the vegetation is snapped or bent by the flow and submerged, the movement of the floats becomes more uniform, leading to improved accuracy in observed discharge. Therefore, when computationally obtaining the discharge hydrograph, we emphasized —and attempted to re-create—observed discharge between its peak in the rising-water period through the receding-water period. Figure 7 graphs observed and calculated discharge for the 3.5km point (upstream-end discharge observation point) of the Watarase River, as well as calculated discharge at the 0.0 km point (downstream end) and the 1.0 km point. The data indicate a forward flow in the Watarase River during the rising-water period, despite a negative water surface slope due to the strong effects of the Tone River.

This indicates that the energy gradient of the flood flow in the Watarase River was positive. At hour 0, discharge at the 0.0 km point was low—the flow was nearly stagnant. Thus, because of the effects of the Tone River, discharge decreased at a slow rate from peak discharge through the receding-water period, lengthening the flood duration.

4.3 Comparison of Storage Volumes

This section concerns storage volume in a section (130.0–138.5 km) of the Tone River. Figure 8 shows that the calculations of the average water level in the river section accurately re-create the observed average water level at 2-hour intervals. Multiplying the change in water level in Figure 8 by the water surface area yields storage volume S for each point in time. Time-differentiating S yields storage volume per unit time (dS/dt). Figure 9 shows temporal change in average storage rate in the section at 2-hour intervals as determined from the data in Figure 8; also shown are the differences between observed and calculated discharge at the upstream and downstream ends. As can be seen in Figure 9, storage rates (dS/dt) determined from observed and calculated water surface profile are essentially the same as storage rates determined from calculated discharge differences ($Q_{in} - Q_{out}$). Storage rates determined from observed discharge differences ($Q_{in} - Q_{out}$) differ considerably from storage rates (dS/dt) determined from water surface profile because of the error in observed discharge, which results in large error in both differences.

To determine the decrease in peak discharge, methods that track temporal change in water surface profile produce better accuracy than methods that use observed discharge at the upstream and downstream ends. In an 8.5 -km section of the Tone River containing the confluence with the Watarase River,

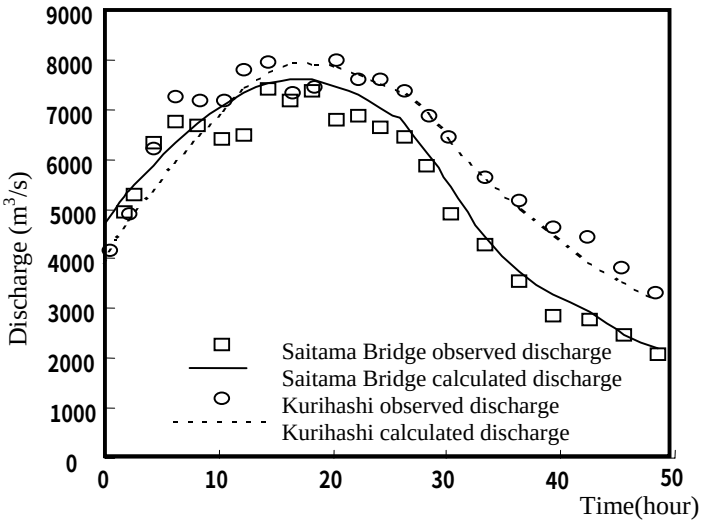

Figure 6. Observed and calculated discharge in the Tone River.

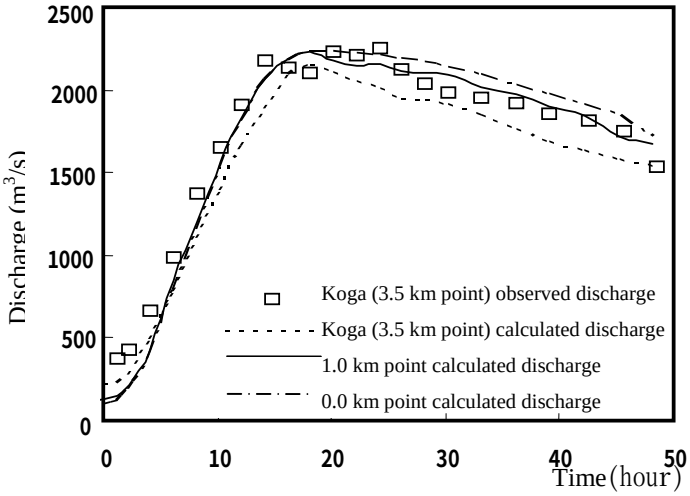

Figure 7. Observed and calculated discharge in the Watarase River.

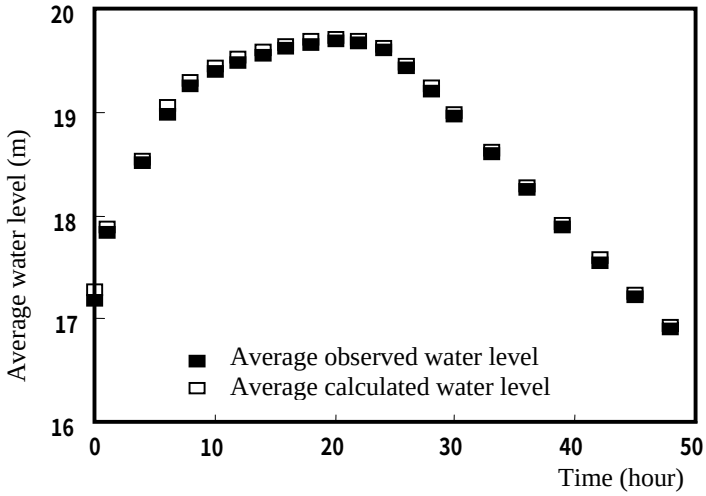

Figure 8. Temporal change in section-averaged water level in the Tone River studied section.

calculated dS/dt was approximately 1,030 m^3/s at peak, meaning that roughly 20% of the discharge entering this section at this time was being stored. Fig. 10—the Watarase River storage rate as calculated from $Q_{in} - Q_{out}$, along with storage rate calculated from observed and calculated water surface profile—shows that dS/dt calculated from observed and calculated water surface profile is roughly equal to the storage rate calculated from the computationally obtained $Q_{in} - Q_{out}$. In short, the calculations properly re-create storage in a confluence where the water surface profile exhibits a negative water surface slope. At peak flooding, the calculated value of dS/dt in the 3.5 -km section of the Watarase River was roughly $330m^3/s$, indicating that an amount of water equivalent to 51% of the discharge entering the section at this time was stored in the channel. Although the September 2001 flooding exhibited such storage properties, other floods occurring in the Tone and Watarase Rivers must be similarly studied.

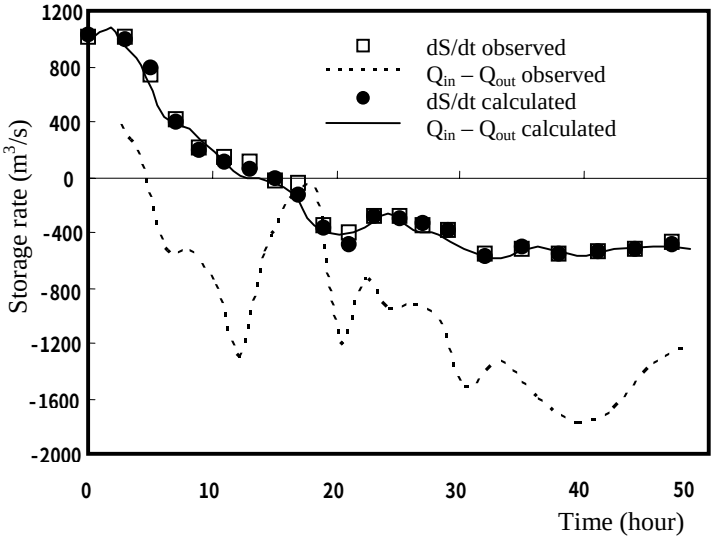

Figure 9. Temporal changes in average storage rate in the observed section (130.0-138.5km) of the Tone River.

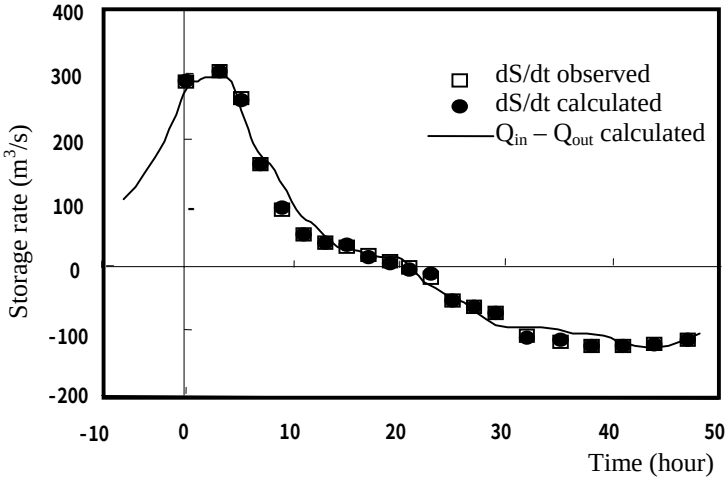

Figure 10. Temporal changes in storage rate in the observed section (0-3.5km) of the Watarase River

5. CONCLUSION

The authors used a combination of field data and computations to derive discharge hydrographs and channel storage volumes for the confluence between the Tone and Watarase Rivers. The primary conclusions reached in this research are as follows.

(1)Using detailed observed water surface profile data, the authors were able to estimate, with a high degree of accuracy, the discharge hydrograph for a confluence having a negative water surface slope in an early stage of rising water period by performing two-dimensional unsteady-flow analysis that conformed to the observed water surface profile. In addition, the calculated discharge hydrograph made it possible to estimate changes in storage volume in the channel. Furthermore, the particular Watarase River flood examined was characterized by a negative water surface slope in the rising-water period due to the large flood discharge, although the flow itself was a forward one.

(2) In the Tone River section—a straight section that confluences with the Watarase River—storage peaked at approximately 20% of the discharge entering the section at that time. In addition, storage was greater in the section of the Watarase River affected by the Tone River.

ACKNOWLEGEMENTS

The authors express our appreciation of the assistance rendered us by Mr. S, Nagai, graduate student of Hiroshima University.

REFERENCES

Fukuoka, S., Watanabe, A., Seki, K., Kurisu, D., and Tokioka, K. (2003). "Assessment and Mechanism of Flood Flow Storage in Channels", Journal of Hydraulic, Coastal and Environmental Engineering, JSCE, No.740/II-64, pp.31-44.

Fukuoka, S., Watanabe, A., Hara, T., and Akiyama, M. (2004a). "Highly Accurate Estimation of Hydrograph of Flood Discharge and Water Storage in Rivers by Using an Unsteady Two-Dimensional Flow Analysis Based on Temporal Change in Observed Water Surface Profiles", Journal of Hydraulic, Costal and Environmental Engineering, JSCE, No.761/Ⅱ-67, pp.45-56.

Fukuoka,S., Watanabe,A.,and Nagai,S. (2004b). "A Water Level Observation for a Flood Storage Estimation in Rivers and Influence of Unsteadiness of Flow on Roughness Coefficient", Journal of Advances in River Engineering, JSCE, Vol.10, pp71-88.

Fukuoka, S. (2005). Flood Hydraulics and Channel Design, Morikita Publishing Company.

Nomitsu,K. (1969). New Potamology, Chijin Shokan Publishing Company.